Clickable Azide-functionalized Bromo-Aryl-Aldehydes – Synthesis and Photophysical Characterization

Dominik Göbel[1], Marius Friedrich[1,2], Enno Lork[3], Boris J. Nachtsheim*[1]

Address: [1]Institute for Organic and Analytical Chemistry, University of Bremen, Leobener Straße 7, D-28359 Bremen, Germany, [2]Department of Organic Chemistry, Technical University Kaiserslautern, Erwin-Schrödinger-Straße Geb.54, D-67663 Kaiserslautern, Germany [3]Institute for Inorganic and Crystallographic Chemistry, University of Bremen, Leobener Straße NW2, D-28359 Bremen, Germany

Email: Boris J. Nachtsheim – nachtsheim@uni-bremen.de

* Corresponding author

Abstract

Herein we present the facile synthesis of three azide-functionalized fluorophores and their covalent attachment as triazoles in Huisgen-type cycloaddition with model alkynes. Besides two *ortho*- and *para*-bromo-substituted benzaldehydes, the azide functionalization of a fluorene-based structure will be presented. The copper(I)-catalyzed azide-alkyne cycloaddition (CuAAC) of the so synthesized azide-functionalized bromocarbaldehydes with terminal alkynes exhibiting different degree of steric demand was performed in high efficiency. Finally, we investigated the photophysical properties of the azide-functionalized arenes and their covalently linked

triazole derivatives to gain deeper insight towards the effect of these covalent linkers on their emission behavior.

Keywords

fluorenes, bromo-arylaldehydes, click-chemistry, phosphorescence, fluorescence

Introduction

Small organic luminophores exhibiting room-temperature phosphorescence (RTP) have attracted great attention due to promising applications in optoelectronic devices [1–8], biological imaging [9–12] and chemical sensing [13–15]. Referring to the Jablonski diagram (see Scheme 1a) [16, 17], upon excitation from the singlet ground state (S_0) to higher singlet states (S_n), followed by internal conversion (IC), either non-radiative or radiative decay to S_0 can occur. While the latter decay (fluorescence) takes place without change in electron spin, phosphorescence is defined as the radiative transition from the lowest excited triplet state (T_1) to the singlet ground state (S_0) [18–21]. Triplet state excitons are generated by the spin-forbidden intersystem crossing (ISC) process from the first excited singlet state (S_1). Pursuant to the El-Sayed rule (see Scheme 1b) [22, 23], ISC is spin allowed from $^1(\mathrm{n}, \pi^*)$ to $^3(\pi, \pi^*)$ and from $^1(\pi, \pi^*)$ to $^3(\mathrm{n}, \pi^*)$ excited states, while ISC is spin-forbidden from $^1(\mathrm{n}, \pi^*)$ to $^3(n, \pi^*)$ and from $^1(\pi, \pi^*)$ to $^3(\pi, \pi^*)$ excited states, owing to poor orbital overlap, resulting in decreased spin-orbit coupling.

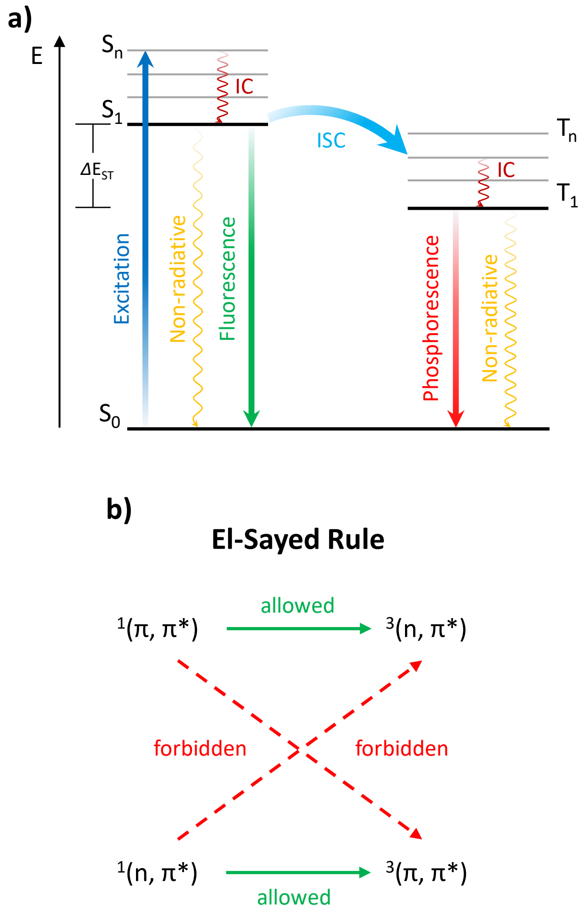

Scheme 1: a) Schematic depiction of the Jablonski diagram; b) Schematic representation of El-Sayed's rule.

Quenching processes of triplet states, induced by molecular motions, oxygen or humidity, restrict the versatile application of such organic materials [24]. Thus, low temperatures [25–27] or inert conditions [28] are necessary to facilitate afterglow emission.

Most phosphorescence studies are focused on metal complexes, due to a strong heavy atom-induced spin-orbit coupling [29–33]. Considering the high price and potential of toxicity of many metal-complexes, pure organic phosphors are highly desirable [16, 17, 34–37]. Two approaches are applied to achieve organic phosphors. (1) Introduction of non-metal heavy atoms such as halogens (Br or I) or functionalities containing lone pairs, in particular carbonyls, nitrogen, sulfur and phosphorus derivatives which facilitate the ISC process from S_1 to T_n and thus increase the spin-orbital coupling [38–47]. Also, decreasing the singlet-triplet splitting energy (ΔE_{ST}) caused by intramolecular charge-transfer (ICT) interactions is an approved method [48, 49]. (2) Significant reduction of nonradiative transitions can be achieved by the host-guest method [50–52] or by crystallization [53–57]. In difference to liquid phase, the highly ordered packing and the restriction of molecular motions in the crystalline state favor persistent luminescence.

The promotion of ISC processes through intermolecular halogen bonding to generate efficient RTP was initially investigated by Kim *et al*. [58]. They developed the minimalistic 2,5-dihexyloxy-4-bromobenzaldehyde **1** [59–63] which shows weak fluorescence in solution, but exhibits green phosphorescence with a quantum yield of Φ_P = 2.9% in the crystalline state: This behavior is caused by intermolecular halogen bonds from the carbonyl-oxygen to an adjacent bromine-atom (Figure 1a).

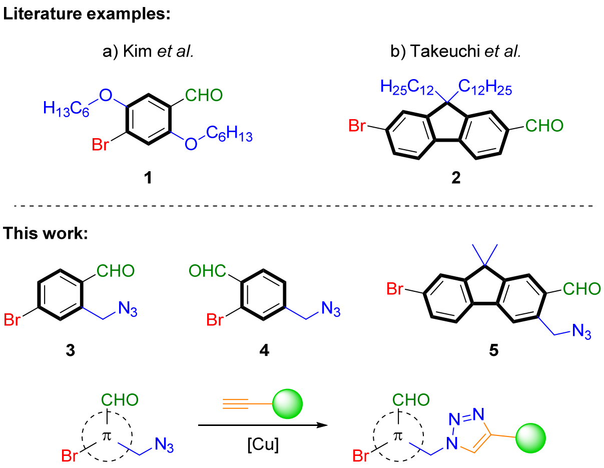

Figure 1: Top: Literature examples of organic compounds showing RTP in the crystalline state (a) and in solution (b). Bottom: Azide-linked derivatives presented in this work.

Despite multifarious examples of RTP in the crystalline state, purely organic compounds showing RTP in solution are rare [64–69]. Takeuchi *et al*. [28] reported a bromofluorenecarbaldehyde **2** which shows blue fluorescence in chloroform at 298 K under air and green phosphorescence under argon with a phosphorescence quantum yield of $\Phi_P = 5.9\%$ (Figure 1b). This observation is reasoned by a strong (π, π^*) character of the T_2-state.

Although phosphorescent organic compounds are well investigated towards their photophysical properties in the crystalline state, in solution or physically embedded in polymer matrices, there is a significant lack of possibilities [61] for their targeted covalent attachment to higher structures. This is due to missing synthetic strategies to incorporate suitable linkable functionalities into those luminophores.

Our group is highly interested in the *de novo* synthesis of small organic luminophores and in this regard we recently developed efficient methods for the synthesis of ESIPT-based luminophores [70, 71]. Herein, we present the efficient functionalization of derivatives of the potent luminophores **1** and **2** with “clickable” azide functionalities to target structures **3-5** and further investigated the influence of this functionalization, both in the unlinked azide state and the linked triazole state, on the emission properties of these compounds (Figure 1).

Results and Discussion

Syntheses

para- and *ortho*-Bromobenzaldehyde 3 and 4

We initiated our synthetic investigations towards azide-functionalized *para*-bromobenzaldehyde **3** in a two-step sequence. Condensation with 2-amino-2-methylpropan-1-ol and oxidation with NBS yielded the oxazoline **6** in good yield. Directed *ortho*-metalation utilizing TMPMgCl·LiCl under mild conditions and subsequent smooth formylation with DMF afforded benzaldehyde **7**. Due to rapid decomposition of **7** under ambient and acidic conditions, rapid aqueous work-up was conducted, followed by reduction with $NaBH_4$, yielding the corresponding primary alcohol **8** in 81% over two steps. The transformation to azide **9** was accomplished by deprotonation using 1,8-diazabicyclo[5.4.0]undec-7-ene (DBU) and reaction with diphenylphosphoryl azide (DPPA) in excellent yield. Finally, the oxazoline group, which acted as directing and protecting group, was removed in a three-step sequence of *N*-methylation, reduction of the *in situ* formed iminium ion and acidic hydrolysis. This afforded the azide-functionalized *para*-bromobenzaldehyde **3** in 78% yield and an overall yield of 56% (starting from 4-bromobenzaldehyde).

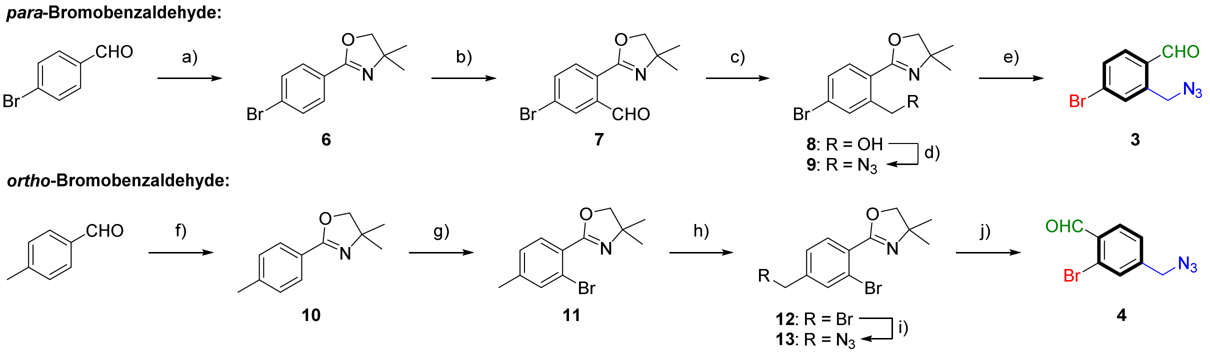

Scheme 2: Reaction conditions: ***para*-Bromobenzaldehyde 3:** a) 1) 2-amino-2-methylpropan-1-ol, 4 Å MS, CH_2Cl_2, 25 °C, 18 h; 2) NBS, CH_2Cl_2, 25 °C, 5 h, 91%; b) 1) TMPMgCl·LiCl, THF, 25 °C, 4 h; 2) DMF, THF, 0 °C to 25 °C, 1.5 h; c) $NaBH_4$, THF:MeOH 1:1, 0 °C, 1 h, 81% (2 steps); d) DPPA, DBU, PhMe, 25 °C, 18 h, 98%; e) 1) MeOTf, CH_2Cl_2, 25 °C, 2.5 h; 2) $NaBH_4$, THF:MeOH 4:1 v:v, 0 °C, 2.5 h; 3) oxalic acid, THF:H_2O 4:1 v:v, 25 °C, 20 h, 78%. Overall yield from 4-bromobenzaldehyde to **3**: 56% (5 steps). ***ortho*-Bromobenzaldehyde 4:** f) 1) 2-amino-2-methylpropan-1-ol, 4 Å MS, CH_2Cl_2, 25 °C, 18 h; 2) NBS, CH_2Cl_2, 25 °C, 4 h, 98%; g) 1) TMPMgCl·LiCl, THF, 25 °C, 4 h; 2) $(CBrCl_2)_2$, THF, 0 °C to 25 °C, 10 h, 76%; h) NBS, AIBN, CCl_4, 100 °C, 7 h, 66%; i) NaN_3, DMF, 25 °C, 4 h, 99%; j) 1) MeOTf, CH_2Cl_2, 25 °C, 2.5 h; 2) $NaBH_4$, THF:MeOH 4:1 v:v, 0 °C, 2.5 h; 3) oxalic acid, THF:H_2O 4:1 v:v, 25 °C, 20 h, 85%. Overall yield from 4-methylbenzaldehyde to **4**: 41% (5 steps).

Azide-functionalized *ortho*-bromobenzaldehyde **4** was prepared by a similar route as aldehyde **3**. Initially, oxazoline formation from 4-methylbenzaldehyde yielded 2-aryloxazoline **10** in almost quantitative yield. Introduction of the *ortho*-bromine substituent was again accomplished by metalation using TMPMgCl·LiCl and subsequent reaction with 1,2-dibromotetrachloroethane to afford **11** in 76% yield. A second bromination at benzylic position provided the dibrominated derivative **12** in 66% yield. Substitution reaction of benzyl bromide with sodium azide delivered primary azide **13** in quantitative yield. Again, final back-conversion of the oxazoline group to the corresponding aldehyde afforded azide-functionalized *ortho*-bromobenzaldehyde **4** in 85% yield and an overall yield of 41% (starting from 4-methylbenzaldehyde).

Bromofluorenecarbaldehyde 5

The synthetic route to azide-functionalized 7-bromofluorene-2-carbaldehyde **5** started from unfunctionalized fluorene. Double bromination to **14**, followed by double methylation of the methylene bridge to **15** and a lithiation/formylation sequence afforded 7-bromofluorene-2-carbaldehyde **16** in excellent yield over three steps. Conversion to the 2-aryloxazoline **17** was accomplished in 92% yield using the same method as described for the synthesis of **6** and **10**. *ortho*-Metalation with TMPMgCl·LiCl [70] and conversion of the magnesiated species with DMF to carbaldehyde **18** was followed by reduction with $NaBH_4$ to give the primary alcohol **19**. In contrast to benzaldehyde **7**, carbaldehyde **18** showed no decomposition at ambient temperature. While acidic hydrolysis of **19** provided exocyclic *γ*-lactone **20**, substitution reaction with DPPA/NaN_3 yielded the primary azide in 87% yield. In accordance to previous deprotection reactions, fluorene **21** was converted by means of a three-step sequence to the desired azide-functionalized 7-bromofluorene-2-carbaldehyde **5** in 86% yield and an overall yield of 45% (starting from fluorene). The molecular structure of **5** could be verified by X-ray diffraction (XRD, see Scheme 3).

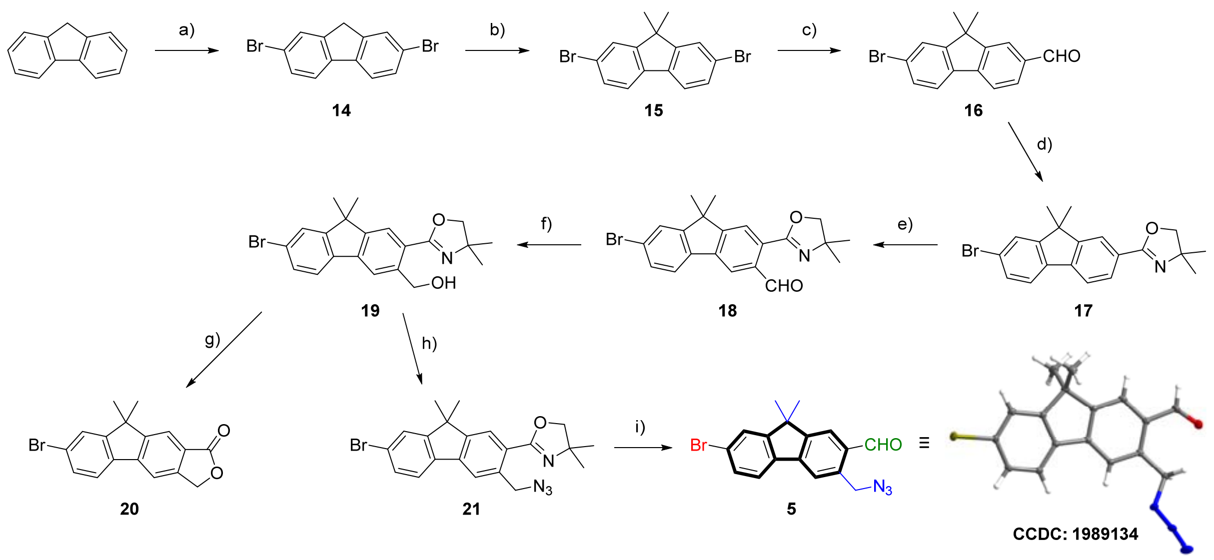

Scheme 3: Reaction conditions: a) Br_2, Fe-powder, $CHCl_3$, 0 °C, 4 h, 99%; b) KOH, KI, MeI, DMSO, 25 °C, 18 h, 92%; c) 1) *n*BuLi, THF, –78 °C, 1 h; 2) DMF, THF, –78 °C to 25 °C, 10 h, 90%; d) 1) 2-amino-2-methylpropan-1-ol, 4 Å MS, CH_2Cl_2, 25 °C, 18 h; 2) NBS, CH_2Cl_2, 25 °C, 3 h, 92%; e) 1) TMPMgCl·LiCl, THF, 25 °C, 4 h; 2) DMF, THF, –15 °C to 25 °C, 2 h; f) $NaBH_4$, THF:MeOH 1:1 v:v, 0 °C, 1.5 h, 79% (2 steps); g) HCl (4 N), 120 °C, 6 h, 91%; h) 1) DPPA, DBU, PhMe, 25 °C, 15 h; 2) NaN_3, PhMe, 60 °C, 4 h, 87%; i) 1) MeOTf, CH_2Cl_2, 25 °C, 2.5 h; 2) $NaBH_4$, THF:MeOH 4:1 v:v, 0 °C, 2.5 h; 3) oxalic acid, THF:H_2O 4:1 v:v, 25 °C, 20 h, 86%. Overall yield to **5**: 45% (8 steps). The molecular structure of **5** shows 50% probability ellipsoids.

Derivatization of fluorenyl methanol 19

To gain deeper insights about the emission behavior of fluorenes bearing different functional groups in the side chains, fluorenyl methanol **19** was subjected to derivatization reactions. Deprotonation and subsequent methylation afforded methoxy derivative **22**, which was then converted into the methoxy-functionalized 7-bromofluorene-2-carbaldehyde **23** in 75% yield. Implementation of potent leaving groups in the side chain as complement linkable functionalities *via* S_N-reaction was initiated by mesylation. Unfortunately, the mesylated fluorene showed such a high reactivity that rapid decomposition occurred. However, bromination was conducted by various substitution methods delivering benzyl bromide **24**, which upon isolation cyclized to iminium bromide **25** in high yields. To suppress this unexpected cyclization, careful fine-adjustment of the work-up conditions were made. Here, upon complete formation of **24**, rapid filtration of the reaction mixture through a plug of neutral alumina, solvent evaporation and quick conversion in the next step was successfully applied. Deprotection to the carbaldehyde was performed using the well applied three-step methylation/reduction/hydrolysis sequence. Methylation of the oxazoline nitrogen afforded iminium salt **26**, which was reduced to oxazolidine **27**. Again, similar to **25**, cyclization took place and ammonium triflate **28** was isolated in 56% yield (starting from **24**). In contrast to the cyclization of oxazoline **24**, oxazolidine **27** cyclized already during the reaction, caused by the increased basicity of the ring nitrogen.

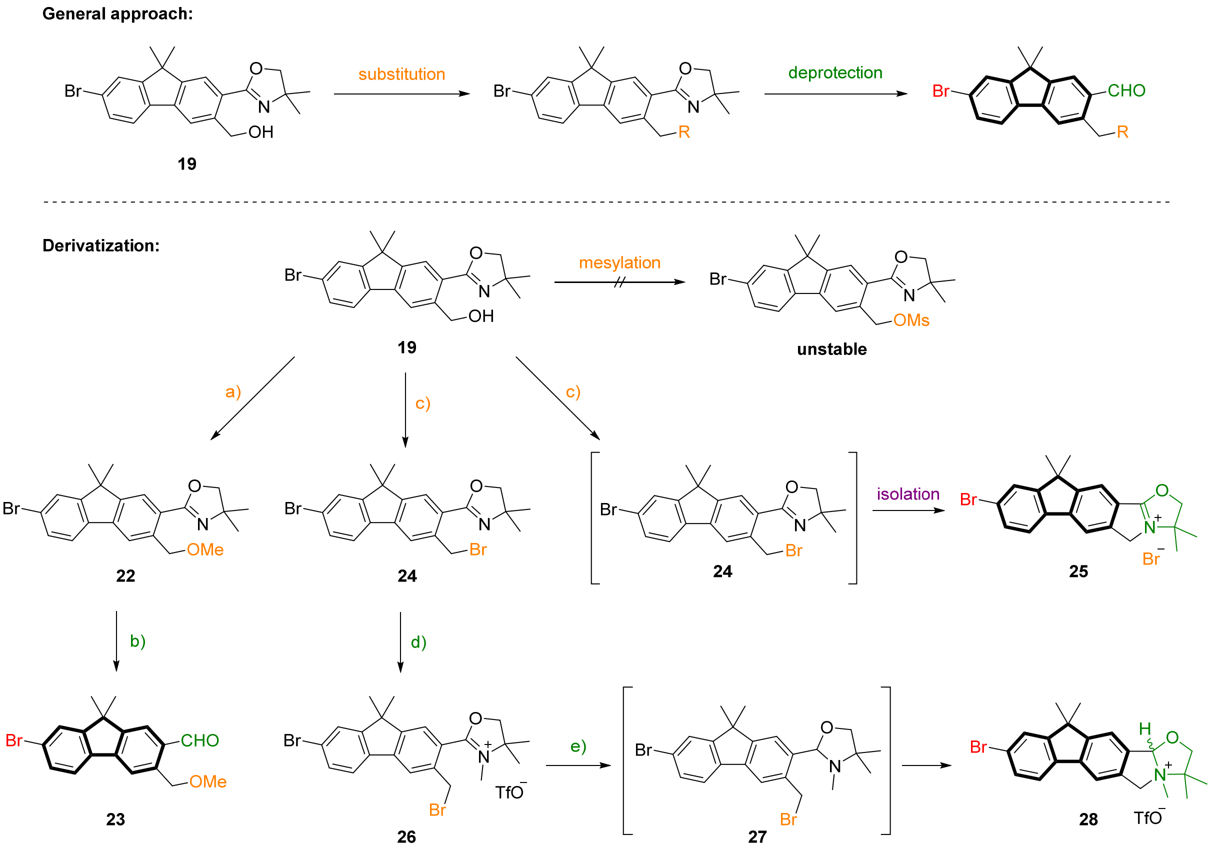

Scheme 4: Reaction conditions: a) 1) NaH, THF, 0 °C, 30 min; 2) MeI, THF, 0 °C to 25 °C, 2 h, 99%; b) 1) MeOTf, CH_2Cl_2, 25 °C, 3 h; 2) $NaBH_4$, THF:MeOH 4:1 v:v, 0 °C, 3 h; 3) oxalic acid, THF:H_2O 4:1 v:v, 25 °C, 24 h, 75%. Overall yield from fluorene to **23**: 44% (8 steps). c) CBr_4, PPh_3, CH_2Cl_2, 0 °C to 25 °C, 2 h, 95%; or NBS, PPh_3, CH_2Cl_2, 0 °C to 25 °C, 2 h, 91%; or PBr_3, CH_2Cl_2, 0 °C to 25 °C, 2 h, 92%; d) MeOTf, CH_2Cl_2, 25 °C, 3 h; e) $NaBH_4$, THF:MeOH 4:1 v:v, 0 °C, 3 h. Overall yield from **24** to **28**: 56% (2 steps).

CuAAC reactions of bromocarbaldehydes

We further investigated the reactivity of azide-functionalized bromocarbaldehydes **3**, **4** and **5** in copper(**I**)-catalyzed azide-alkyne cycloaddition reactions (CuAAC). For this, we treated the azide-functionalized luminophores with alkynes exhibiting different degree of steric demand, including 1-decyne **29**, phenyl acetylene **30**, 1-ethynyladamantane **31** and 1,3-di-*tert*-butyl-5-ethynylbenzene **32** (see Scheme 5). All triazoles **33**-**44**, based on the bromocarbaldehydes **3**, **4** and **5** were successfully isolated in excellent yields of > 90%. As a further model functionalization, the sterically demanding adamantly substituted triazole **42** was subjected to a methylation reaction with Meerwein's salt (trimethyloxonium tetrafluoroborate) to deliver the *N*-methylated triazole **45** in 83% yield.

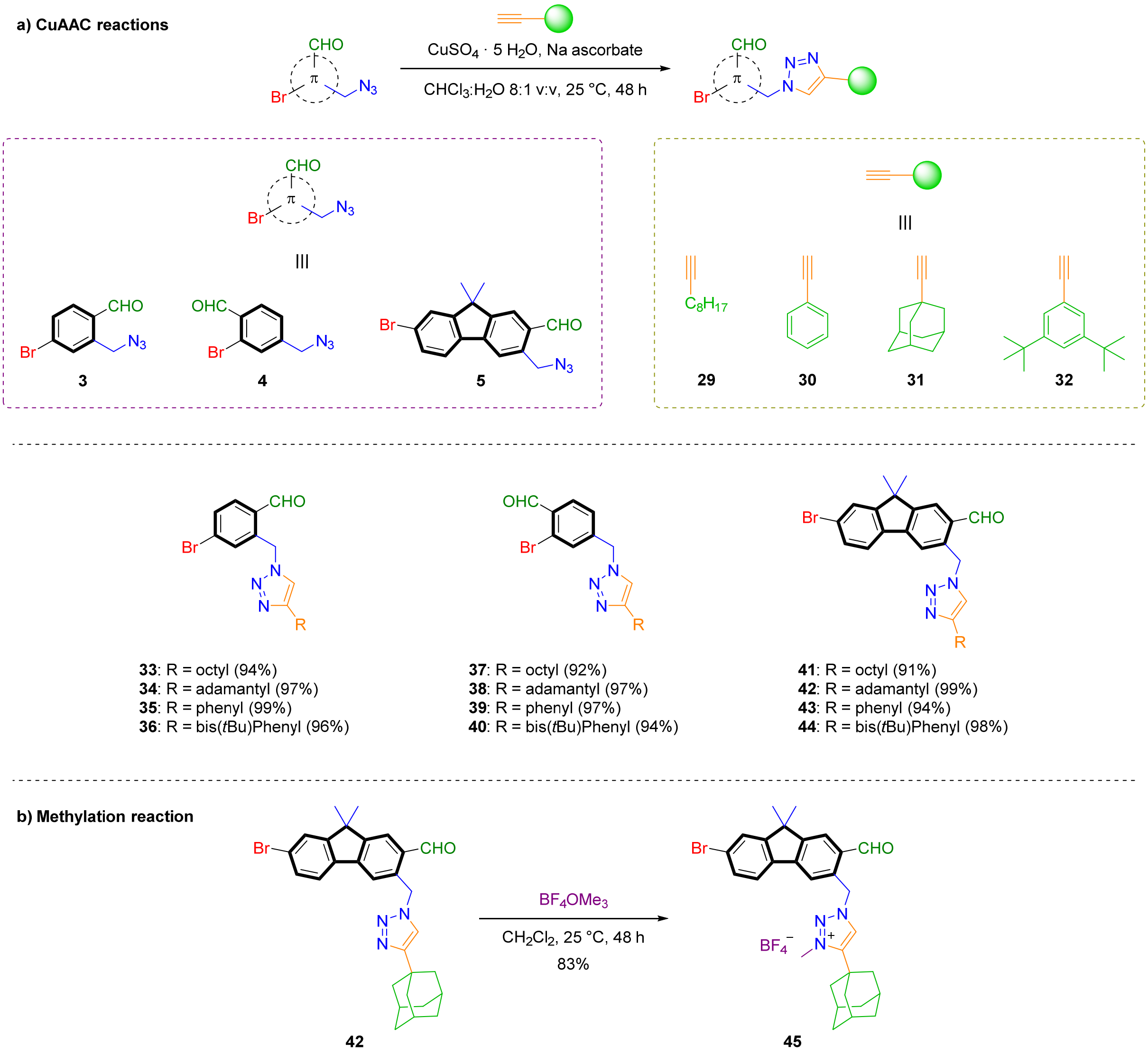

Scheme 5: a) CuAAC reactions of azide-functionalized bromocarbaldehydes **3**, **4** and **5** with terminal alkynes to triazoles **33-44**. General reaction conditions for CuAAC reactions: Azide (1.00 eq), terminal alkyne (1.05 eq), $CuSO_4 \cdot 5\ H_2O$ (0.1 eq), Na ascorbate (0.50 eq), $CHCl_3$, (0.1 M) and water (12.5 mM) at 25 °C for 48 h. b) Methylation reaction of adamantly substituted triazole **42** with Meerwein's salt (trimethyloxonium tetrafluoroborate).

Photophysical properties

We finally examined the photophysical properties of both the azides and the triazoles. UV-Vis absorption measurements of *para*-Bromobenzaldehyde **3** and *ortho*-

Bromobenzaldehyde **4** as well as the corresponding triazoles **33**-**40** were conducted in chloroform. Intense absorption bands below 270 nm are observed, which can be attributed to typical *π*-*π** transitions deriving from the single-benzene core. In addition, unstructured absorption bands above 290 nm are observed, while *ortho*-derivatives exhibit more broadened bands than the *para*-derivatives (see Figure 2a and S1-S11). Emission spectra for *para*-bromocarbaldehyde **3** and adamantyl-triazole **34** in the solid-state show maxima at 440 nm (for compound **3**) and 416 nm (for compound **34**) (see Figure 2b). Additionally, fluorescence half lifetimes (*τ*) of **3** and **34** were determined by time correlated single photon counting (TCSPC), indicating low half-lifetimes of 2.21 ns (for compound **3**) and 3.23 ns (for compound **34**) for lower populated species (see Figure S6). Quantum yields (*Φ*) of both derivatives are below 1% in the solid-state. In chloroform no luminescence was detected for the *para*-derivatives. All *ortho*-derivatives exhibit no luminescence neither in solution nor in the solid-state [72].

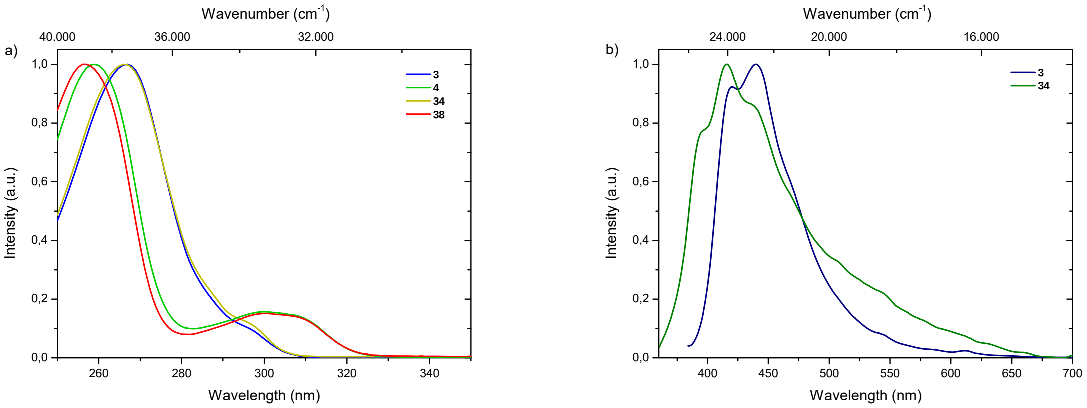

Figure 2: a) Normalized UV-Vis absorption spectra of **3** (blue line), **34** (green line), **4** (yellow line) and **38** (red line) in $CHCl_3$. b) Normalized emission spectra of **3** (navy line), **34** (olive line) in $CHCl_3$ after bubbling with argon for 30 minutes.

These observations for *para*- and *ortho*-bromobenzaldehydes indicate that phosphorescence is quenched in these systems yielding only weak fluorescence. This may be owing to the azide-moiety either as functional group or as part of the triazole heterocycle. Similar observations were already made on luminescent materials [73, 74].

Fluorene derivatives were subjected to photophysical measurements as well. UV-Vis absorption spectra of bromofluorenecarbaldehydes **5** and **16** show intense absorption bands at 331 and 330 nm. Furthermore, adamantyl-triazole **42** and the corresponding tetrafluoroborate salt **45** exhibit similar absorption properties, while the methylated species **45** shows a comparable slightly red-shifted absorption band (see Figure 3a and S12-S14). Emission measurements of carbaldehydes **5** and **16** reveal that solid-state emission bands are more blue-shifted than emission bands in solution (see Figure 3b). Similar observations were made for adamantyl-triazole **42** and tetrafluoroborate salt **45** with maxima at 510 nm and 540 nm (see Figure 3c). However, TCSPC demonstrate that solely fluorescence is observed in all physical states for all investigated compounds with a maximum half-lifetime τ of 11.6 ns for methylated triazole **45** in chloroform (see Figure 3d). Quantum yields Φ were determined to be < 1% for all structures. Further fluorene derivatives – methoxymethyl carbaldehyde **23**, iminium bromide **25** and ammonium triflate **28** – exhibit intense absorption maxima around 320 nm (see Figure S13). For **25** and **28**, emission maxima in the solid-state were red-shifted compared to emission bands in chloroform solution (see Figure S31 and S33). **23** Exhibits a deep violet emission maximum at 360 nm in chloroform solution and no emission in the solid-state (see Figure S30). Half-lifetimes τ were defined up to 8.66 ns for iminium bromide **25**, with quantum yields Φ below 1% (see Figure S32). The absence of any long living triplet species in all fluorene derivatives in solution as well as in the solid-state again indicates undesirable quenching events induced by the azide functionalities, similar to *para*- and *ortho*-bromobenzaldehydes.

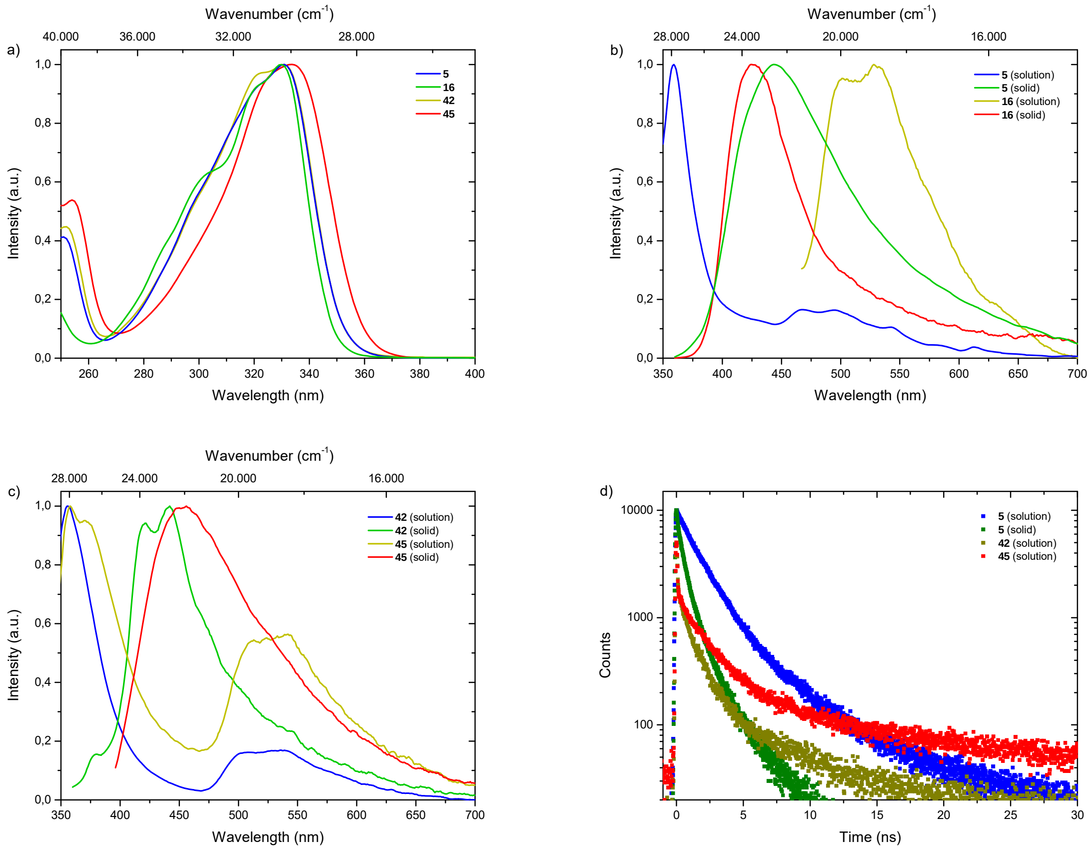

Figure 3: a) Normalized UV-Vis absorption spectra of **5** (blue line), **16** (green line), **42** (yellow line) and **45** (red line) in $CHCl_3$. b) Normalized emission spectra of **5** (in solution, blue line and solid-state, green line) and **16** (in solution, yellow line and solid-state, red line). c) Normalized emission spectra of **42** (in solution, blue line and solid-state, green line) and **45** (in solution, yellow line and solid-state, red line). d) Time resolved emission decay curves of **5** (in solution, blue dots and solid-state, green dots), **42** (in solution, yellow dots) and **45** (in solution, red dots) at 25 °C. In all diluted measurements (c = 10^{-5} mol · L^{-1}) $CHCl_3$ was used as solvent and solutions were sparged with argon for 30 minutes.

Conclusion

In summary, azide-functionalized *ortho*- and *para*-bromo benzaldehydes and fluorene derivates were successfully synthesized. The azide bearing arenes were efficiently linked with even sterically highly demanding alkynes in a copper(I)-catalyzed azide-alkyne cycloaddition (CuAAC). Initial photophysical investigations of azide-functionalized bromocarbaldehydes and fluorenes revealed that the azide-moiety and the triazole heterocycle efficiently quench phosphorescent transitions. Efforts of installing other functional groups suitable for covalent connections or modification of the alkyl bridge between the arene and the azide are underway in our laboratories.

Supporting Information

Supporting Information File 1:

Detailed experimental procedures, characterization data, photophysical properties, and copies of NMR spectra.

Supporting Information File 2:

Crystallographic data for compound **5**.

Acknowledgements

We thank Prof. Dr. Nadja-C. Bigall, Dr. Dirk Dorfs and Pascal Rusch (all from Leibniz University Hannover) for supporting the photophysical measurements.

References

1. Kabe, R.; Notsuka, N.; Yoshida, K.; Adachi, C. *Adv. Mater.* **2016**, *28*, 655–660. doi:10.1002/adma.201504321

2. Tao, Y.; Yang, C.; Qin, J. *Chem. Soc. Rev.* **2011**, *40*, 2943–2970. doi:10.1039/c0cs00160k
3. Goushi, K.; Yoshida, K.; Sato, K.; Adachi, C. *Nat. Photonics* **2012**, *6*, 253–258. doi:10.1038/nphoton.2012.31
4. Zhang, Q.; Li, B.; Huang, S.; Nomura, H.; Tanaka, H.; Adachi, C. *Nat. Photonics* **2014**, *8*, 326–332. doi:10.1038/nphoton.2014.12
5. Chaudhuri, D.; Wettach, H.; van Schooten, K. J.; Liu, S.; Sigmund, E.; Höger, S.; Lupton, J. M. *Angew. Chem. Int. Ed.* **2010**, *49*, 7714–7717. doi:10.1002/anie.201003291
6. Chaudhuri, D.; Sigmund, E.; Meyer, A.; Röck, L.; Klemm, P.; Lautenschlager, S.; Schmid, A.; Yost, S. R.; van Voorhis, T.; Bange, S.; Höger, S.; Lupton, J. M. *Angew. Chem. Int. Ed.* **2013**, *52*, 13449–13452. doi:10.1002/anie.201307601
7. Murawski, C.; Leo, K.; Gather, M. C. *Adv. Mater.* **2013**, *25*, 6801–6827. doi:10.1002/adma.201301603
8. Baldo, M. A.; O'Brien, D. F.; You, Y.; Shoustikov, A.; Sibley, S.; Thompson, M. E.; Forrest, S. R. *Nature* **1998**, *395*, 151–154. doi:10.1038/25954
9. Gao, R.; Mei, X.; Yan, D.; Liang, R.; Wei, M. *Nat. Commun.* **2018**, *9*, 2798. doi:10.1038/s41467-018-05223-3
10. Miao, Q.; Xie, C.; Zhen, X.; Lyu, Y.; Duan, H.; Liu, X.; Jokerst, J. V.; Pu, K. *Nat. Biotechnol.* **2017**, *35*, 1102–1110. doi:10.1038/nbt.3987
11. Zhen, X.; Tao, Y.; An, Z.; Chen, P.; Xu, C.; Chen, R.; Huang, W.; Pu, K. *Adv. Mater.* **2017**, *29*, 1606665. doi:10.1002/adma.201606665
12. Zhang, G.; Palmer, G. M.; Dewhirst, M. W.; Fraser, C. L. *Nat. Mater.* **2009**, *8*, 747–751. doi:10.1038/nmat2509
13. DeRosa, C. A.; Seaman, S. A.; Mathew, A. S.; Gorick, C. M.; Fan, Z.; Demas, J. N.; Peirce, S. M.; Fraser, C. L. *ACS Sens.* **2016**, *1*, 1366–1373. doi:10.1021/acssensors.6b00533
14. Lehner, P.; Staudinger, C.; Borisov, S. M.; Klimant, I. *Nat. Commun.* **2014**, *5*, 4460. doi:10.1038/ncomms5460
15. Kwon, M. S.; Lee, D.; Seo, S.; Jung, J.; Kim, J. *Angew. Chem. Int. Ed.* **2014**, *53*, 11177–11181. doi:10.1002/anie.201404490

16. Xiao, L.; Fu, H. *Chem. Eur. J.* **2019**, *25*, 714–723. doi:10.1002/chem.201802819
17. Jia, W.; Wang, Q.; Shi, H.; An, Z.; Huang, W. *Chem. Eur. J.* **2020**, *26*, 4437–4448. doi:10.1002/chem.201904500
18. Kasha, M. *Chem. Rev.* **1947**, *41*, 401–419. doi:10.1021/cr60129a015
19. Lewis, G. N.; Calvin, M. *J. Am. Chem. Soc.* **1945**, *67*, 1232–1233. doi:10.1021/ja01223a513
20. Lewis, G. N.; Kasha, M. *J. Am. Chem. Soc.* **1944**, *66*, 2100–2116. doi:10.1021/ja01240a030
21. Lewis, G. N.; Lipkin, D.; Magel, T. T. *J. Am. Chem. Soc.* **1941**, *63*, 3005–3018. doi:10.1021/ja01856a043
22. S. K. Lower and M. A. El-Sayed; Lower, S. K.; El-Sayed, M. A. *Chem. Rev.* **1966**, *66*, 199–241. doi:10.1021/cr60240a004
23. El-Sayed, M. A. *J. Chem. Phys.* **1963**, *38*, 2834–2838. doi:10.1063/1.1733610
24. Hirata, S. *Adv. Optical Mater.* **2017**, *5*, 1700116. doi:10.1002/adom.201700116
25. Menning, S.; Kramer, M.; Coombs, B. A.; Rominger, F.; Beeby, A.; Dreuw, A.; Bunz, U. H. F. *J. Am. Chem. Soc.* **2013**, *135*, 2160–2163. doi:10.1021/ja400416r
26. Yuan, W. Z.; Shen, X. Y.; Zhao, H.; Lam, J. W. Y.; Tang, L.; Lu, P.; Wang, C.; Liu, Y.; Wang, Z.; Zheng, Q.; Sun, J. Z.; Ma, Y.; Tang, B. Z. *J. Phys. Chem. C* **2010**, *114*, 6090–6099. doi:10.1021/jp909388y
27. Zhang, G.; Chen, J.; Payne, S. J.; Kooi, S. E.; Demas, J. N.; Fraser, C. L. *J. Am. Chem. Soc.* **2007**, *129*, 8942–8943. doi:10.1021/ja0720255
28. Xu, J.; Takai, A.; Kobayashi, Y.; Takeuchi, M. *Chem. Commun.* **2013**, *49*, 8447–8449. doi:10.1039/c3cc44809f
29. Schulze, M.; Steffen, A.; Würthner, F. *Angew. Chem. Int. Ed.* **2015**, *54*, 1570–1573. doi:10.1002/anie.201410437
30. Hirata, S.; Totani, K.; Yamashita, T.; Adachi, C.; Vacha, M. *Nat. Mater.* **2014**, *13*, 938–946. doi:10.1038/nmat4081
31. Pan, Z.; Lu, Y.-Y.; Liu, F. *Nat. Mater.* **2011**, *11*, 58–63. doi:10.1038/nmat3173
32. Tong, B.; Mei, Q.; Wang, S.; Fang, Y.; Meng, Y.; Wang, B. *J. Mater. Chem.* **2008**, *18*, 1636–1639. doi:10.1039/b800977e

33. Liu, Z. W.; Guan, M.; Bian, Z. Q.; Nie, D. B.; Gong, Z. L.; Li, Z. B.; Huang, C. H. *Adv. Funct. Mater.* **2006**, *16*, 1441–1448. doi:10.1002/adfm.200600099
34. Zhao, J.; Chen, K.; Hou, Y.; Che, Y.; Liu, L.; Jia, D. *Org. Biomol. Chem.* **2018**, *16*, 3692–3701. doi:10.1039/c8ob00421h
35. Forni, A.; Lucenti, E.; Botta, C.; Cariati, E. *J. Mater. Chem. C* **2018**, *6*, 4603–4626. doi:10.1039/C8TC01007B
36. Baroncini, M.; Bergamini, G.; Ceroni, P. *Chem. Commun.* **2017**, *53*, 2081–2093. doi:10.1039/c6cc09288h
37. Mukherjee, S.; Thilagar, P. *Chem. Commun.* **2015**, *51*, 10988–11003. doi:10.1039/c5cc03114a
38. Shi, H.; Song, L.; Ma, H.; Sun, C.; Huang, K.; Lv, A.; Ye, W.; Wang, H.; Cai, S.; Yao, W.; Zhang, Y.; Zheng, R.; An, Z.; Huang, W. *J. Phys. Chem. Lett.* **2019**, *10*, 595–600. doi:10.1021/acs.jpclett.8b03712
39. Li, J.-A.; Zhou, J.; Mao, Z.; Xie, Z.; Yang, Z.; Xu, B.; Liu, C.; Chen, X.; Ren, D.; Pan, H.; Shi, G.; Zhang, Y.; Chi, Z. *Angew. Chem. Int. Ed.* **2018**, *57*, 6449–6453. doi:10.1002/anie.201800762
40. Xiong, Y.; Zhao, Z.; Zhao, W.; Ma, H.; Peng, Q.; He, Z.; Zhang, X.; Chen, Y.; He, X.; Lam, J. W. Y.; Tang, B. Z. *Angew. Chem. Int. Ed.* **2018**, *57*, 7997–8001. doi:10.1002/anie.201800834
41. Gu, L.; Shi, H.; Miao, C.; Wu, Q.; Cheng, Z.; Cai, S.; Gu, M.; Ma, C.; Yao, W.; Gao, Y.; An, Z.; Huang, W. *J. Mater. Chem. C* **2018**, *6*, 226–233. doi:10.1039/C7TC04452F
42. Cai, S.; Shi, H.; Zhang, Z.; Wang, X.; Ma, H.; Gan, N.; Wu, Q.; Cheng, Z.; Ling, K.; Gu, M.; Ma, C.; Gu, L.; An, Z.; Huang, W. *Angew. Chem. Int. Ed.* **2018**, *57*, 4005–4009. doi:10.1002/anie.201800697
43. Cai, S.; Shi, H.; Tian, D.; Ma, H.; Cheng, Z.; Wu, Q.; Gu, M.; Huang, L.; An, Z.; Peng, Q.; Huang, W. *Adv. Funct. Mater.* **2018**, *28*, 1705045. doi:10.1002/adfm.201705045
44. Cai, S.; Shi, H.; Li, J.; Gu, L.; Ni, Y.; Cheng, Z.; Wang, S.; Xiong, W.-W.; Li, L.; An, Z.; Huang, W. *Adv. Mater.* **2017**, *29*, 1701244. doi:10.1002/adma.201701244
45. Yang, Z.; Mao, Z.; Zhang, X.; Ou, D.; Mu, Y.; Zhang, Y.; Zhao, C.; Liu, S.; Chi, Z.; Xu, J.; Wu, Y.-C.; Lu, P.-Y.; Lien, A.; Bryce, M. R. *Angew. Chem. Int. Ed.* **2016**, *55*, 2181–2185. doi:10.1002/anie.201509224

46. Gong, Y.; Chen, G.; Peng, Q.; Yuan, W. Z.; Xie, Y.; Li, S.; Zhang, Y.; Tang, B. Z. *Adv. Mater.* **2015**, *27*, 6195–6201. doi:10.1002/adma.201502442

47. An, Z.; Zheng, C.; Tao, Y.; Chen, R.; Shi, H.; Chen, T.; Wang, Z.; Li, H.; Deng, R.; Liu, X.; Huang, W. *Nat. Mater.* **2015**, *14*, 685–690. doi:10.1038/nmat4259

48. Yu, Z.; Wu, Y.; Peng, Q.; Sun, C.; Chen, J.; Yao, J.; Fu, H. *Chem. Eur. J.* **2016**, *22*, 4717–4722. doi:10.1002/chem.201600300

49. Chen, X.; Xu, C.; Wang, T.; Zhou, C.; Du, J.; Wang, Z.; Xu, H.; Xie, T.; Bi, G.; Jiang, J.; Zhang, X.; Demas, J. N.; Trindle, C. O.; Luo, Y.; Zhang, G. *Angew. Chem. Int. Ed.* **2016**, *55*, 9872–9876. doi:10.1002/anie.201601252

50. Lin, Z.; Kabe, R.; Nishimura, N.; Jinnai, K.; Adachi, C. *Adv. Mater.* **2018**, *30*, 1803713. doi:10.1002/adma.201803713

51. Li, D.; Lu, F.; Wang, J.; Hu, W.; Cao, X.-M.; Ma, X.; Tian, H. *J. Am. Chem. Soc.* **2018**, *140*, 1916–1923. doi:10.1021/jacs.7b12800

52. Kabe, R.; Adachi, C. *Nature* **2017**, *550*, 384–387. doi:10.1038/nature24010

53. Gan, N.; Wang, X.; Ma, H.; Lv, A.; Wang, H.; Wang, Q.; Gu, M.; Cai, S.; Zhang, Y.; Fu, L.; Zhang, M.; Dong, C.; Yao, W.; Shi, H.; An, Z.; Huang, W. *Angew. Chem. Int. Ed.* **2019**, *58*, 14140–14145. doi:10.1002/anie.201907572

54. Yang, J.; Ren, Z.; Chen, B.; Fang, M.; Zhao, Z.; Tang, B. Z.; Peng, Q.; Li, Z. *J. Mater. Chem. C* **2017**, *5*, 9242–9246. doi:10.1039/C7TC03656F

55. Shimizu, M.; Shigitani, R.; Nakatani, M.; Kuwabara, K.; Miyake, Y.; Tajima, K.; Sakai, H.; Hasobe, T. *J. Phys. Chem. C* **2016**, *120*, 11631–11639. doi:10.1021/acs.jpcc.6b03276

56. Xie, Y.; Ge, Y.; Peng, Q.; Li, C.; Li, Q.; Li, Z. *Adv. Mater.* **2017**, *29*, 1606829. doi:10.1002/adma.201606829

57. Bergamini, G.; Fermi, A.; Botta, C.; Giovanella, U.; Di Motta, S.; Negri, F.; Peresutti, R.; Gingras, M.; Ceroni, P. *J. Mater. Chem. C* **2013**, *1*, 2717–2724. doi:10.1039/c3tc00878a

58. Bolton, O.; Lee, K.; Kim, H.-J.; Lin, K. Y.; Kim, J. *Nat. Chem.* **2011**, *3*, 205–210. doi:10.1038/nchem.984

59. Yu, Y.; Kwon, M. S.; Jung, J.; Zeng, Y.; Kim, M.; Chung, K.; Gierschner, J.; Youk, J. H.; Borisov, S. M.; Kim, J. *Angew. Chem. Int. Ed.* **2017**, *56*, 16207–16211. doi:10.1002/anie.201708606

60. Kwon, M. S.; Jordahl, J. H.; Phillips, A. W.; Chung, K.; Lee, S.; Gierschner, J.; Lahann, J.; Kim, J. *Chem. Sci.* **2016**, *7*, 2359–2363. doi:10.1039/C5SC03986J

61. Kwon, M. S.; Yu, Y.; Coburn, C.; Phillips, A. W.; Chung, K.; Shanker, A.; Jung, J.; Kim, G.; Pipe, K.; Forrest, S. R.; Youk, J. H.; Gierschner, J.; Kim, J. *Nat. Commun.* **2015**, *6*, 8947. doi:10.1038/ncomms9947

62. Lee, D.; Jung, J.; Bilby, D.; Kwon, M. S.; Yun, J.; Kim, J. *ACS Appl. Mater. Interfaces* **2015**, *7*, 2993–2997. doi:10.1021/am5087165

63. Bolton, O.; Lee, D.; Jung, J.; Kim, J. *Chem. Mater.* **2014**, *26*, 6644–6649. doi:10.1021/cm503678r

64. Goudappagouda; Manthanath, A.; Wakchaure, V. C.; Ranjeesh, K. C.; Das, T.; Vanka, K.; Nakanishi, T.; Babu, S. S. *Angew. Chem. Int. Ed.* **2019**, *58*, 2284–2288. doi:10.1002/anie.201811834

65. Kuila, S.; Rao, K. V.; Garain, S.; Samanta, P. K.; Das, S.; Pati, S. K.; Eswaramoorthy, M.; George, S. J. *Angew. Chem. Int. Ed.* **2018**, *57*, 17115–17119. doi:10.1002/anie.201810823

66. Yu, Z.; Wu, Y.; Xiao, L.; Chen, J.; Liao, Q.; Yao, J.; Fu, H. *J. Am. Chem. Soc.* **2017**, *139*, 6376–6381. doi:10.1021/jacs.7b01574

67. Huang, C.-H.; Wu, P.-J.; Chung, K.-Y.; Chen, Y.-A.; Li, E. Y.; Chou, P.-T. *Phys. Chem. Chem. Phys.* **2017**, *19*, 8896–8901. doi:10.1039/c7cp00074j

68. Ventura, B.; Bertocco, A.; Braga, D.; Catalano, L.; d'Agostino, S.; Grepioni, F.; Taddei, P. *J. Phys. Chem. C* **2014**, *118*, 18646–18658. doi:10.1021/jp5049309

69. Koch, M.; Perumal, K.; Blacque, O.; Garg, J. A.; Saiganesh, R.; Kabilan, S.; Balasubramanian, K. K.; Venkatesan, K. *Angew. Chem. Int. Ed.* **2014**, *53*, 6378–6382. doi:10.1002/anie.201402199

70. Göbel, D.; Clamor, N.; Nachtsheim, B. J. *Org. Biomol. Chem.* **2018**, *16*, 4071–4075. doi:10.1039/c8ob01072b

71. Göbel, D.; Clamor, N.; Lork, E.; Nachtsheim, B. J. *Org. Lett.* **2019**, *21*, 5373–5377. doi:10.1021/acs.orglett.9b01350

72. Sarkar, S.; Hendrickson, H. P.; Lee, D.; DeVine, F.; Jung, J.; Geva, E.; Kim, J.; Dunietz, B. D. *J. Phys. Chem. C* **2017**, *121*, 3771–3777. doi:10.1021/acs.jpcc.6b12027

73. Xie, S.; Proietti, G.; Ramström, O.; Yan, M. *J. Org. Chem.* **2019**, *84*, 14520–14528. doi:10.1021/acs.joc.9b02050

74. Lord, S. J.; Lee, H.-L. D.; Samuel, R.; Weber, R.; Liu, N.; Conley, N. R.; Thompson, M. A.; Twieg, R. J.; Moerner, W. E. *J. Phys. Chem. B* **2010**, *114*, 14157–14167. doi:10.1021/jp907080r